IJE TRANSACTIONS B: Applications Vol. 28, No. 2, (February 2015) 164-171

International Journal of Engineering

Journal Homepage: www.ije.ir

Simulation of Strap-on Boosters Separation in the Atmosphere

M. Jafari*[a], A. Toloei[a], S. Ghasemlu[b], H. Parhizkar[b]

[a]*Department of New Technologies Engineering, Shahid Beheshti University, Tehran, Iran*
[b]*Space Research Institute, Tehran, Iran*

PAPER INFO

Paper history:
Received 04 July 2014
Received in revised form 07 October 2014
Accepted 13 November 2014

Keywords:
Strap-on Boosters Separation
Numerical Dynamic-aerodynamic Interface
Constraint Force Equation Methodology

ABSTRACT

A numerical dynamic-aerodynamic interface for simulating the separation dynamics of constrained strap-on boosters jettisoned in the atmosphere is presented. The aim of the presented interface is to facilitate the simultaneous simulation of complicated dynamic separation mechanisms and full numerical CFD aerodynamic solver. A 6-DOF multi body dynamic solver using Constraint Force Equation Methodology is coupled with a numerical time dependent Euler flow solver. An automatic dynamic mesh updating procedure is employed using smoothing and local remeshing technique. This interface can simulate multi body separation problem by modeling the full separation mechanisms like springs, thrusters, joints and so on, regarding the aerodynamic effects. The flow solver is validated by the Titan-IV launch vehicle experimental data. The proposed simulated separation integration is used for a typical launch vehicle with two strap-on boosters using spring ejector mechanism and spherical constraint joints acting in the dense atmosphere.

***doi**: 10.5829/idosi.ije.2015.28.02b.01*

1. INTRODUCTION

Strap-on boosters are used to increase the payload capabilities of launch vehicles. By adding boosters to the rocket core, the design and manufacturing of launcher becomes more complex. One of the important issues in design and construction of these launchers is the safe booster separation from the core rocket. Any unexpected instability in this sectionor, any catastrophic collision and in general any factor that prevents successful separation, can tend the entire mission to fail. Since the booster separation usually takes place in the dense atmosphere, in addition to the dynamic effect of ejection mechanisms, aerodynamic flow around the launch vehicle is also important. Many researchers have investigated this field for several years. Meakin and Suhs from NASA Ames analyzed the solid rocket booster (SRB) separation of a space shuttle with a Navier–Stokes solver, using a prescribed trajectory for dynamic analysis of body motion [1]. Lochan and Adimurthy analyzed the separation dynamics of strap-on boosters from the core rocket, they used wind tunnel data for the measurement of aerodynamic forces [2]. Lijewski and Suhs developed an unsteady technique for store separation from a delta wing [3]. In addition, Taylor et al. for the Titan IV with two boosters and Azevedo and Moraes for the AVLS launch vehicle with four boosters, carried out similar analyses using steady state aerodynamic without considering the relative motion of boosters [4, 5]. As the first efforts, Kim et al. used dynamic and numerical aerodynamic coupling to simulate strap-on boosters separation [6]. They also studied the effects of flow turbulence in booster separation. In both recent cases, compared to conventional methods for solving separation problems using dynamic mesh method (in aerodynamics) [7], the integrated dynamic code is brief and simple without any complex separation mechanisms. In fact, the simulation is based on the aerodynamic analysis with an integrated simple 6-DOF dynamic code. In other cases, separation mechanisms have to be prescribed in the calculations [7, 8]. Comm-

*Corresponding Author's Email: Mostafa.Jafari.um@gmail.com (M. Jafari)

Please cite this article as: M. Jafari, A. Toloei, S. Ghasemlu, H. Parhizkar, Simulation of Strap-on Boosters Separation in the Atmosphere, International Journal of Engineering (IJE), TRANSACTIONS B: Applications Vol. 28, No. 2, (February 2015) 164-171

ercial flow solvers have been of great interest in separation analysis. FLUENT and OVERFLOW can be considered as good paragon of these solvers that have been frequently mentioned in the literature [7, 9, 10]. Both of these solvers utilized a 6-DOF rigid body motion code with simple and prescribed separation mechanism, which is integrated into the unsteady Navier–Stokes (Euler) solver using an automated grid adoption method.

In the early 2000s to develop the next generation of orbiter with reusability, the separation process was considered as one of the critical technologies [9]. For this purpose, softwares like ConSep, Sepsim using ADAMS (Automatic Dynamic Analysis of Mechanical Systems) solver with aide of wind tunnel results have been developed [10-12]. In such softwares, complex full separation mechanisms can be modeled but large aerodynamic coefficient databases are needed for calculation of aerodynamic effects on booster separation. In 2006, Pamadi et al. at NASA have examined the shuttle booster separation using Concep software and wind tunnel results [9]. In addition, this work has been done by the CFE/POST2 software [13].

This paper is focused on developing a dynamic/ aerodynamic coupled solver to simulate strap-on boosters separation using constraint dynamics and time dependent CFD. Therefore, two commercial solvers i.e. MscADAMS and FLUENT are integrated together with an innovative MATLAB/SIMULINK interface to constitute a powerful package that presents real time dynamic/aerodynamic coupled analysis. Independence of dynamic and aerodynamic solvers, allows the modeling of any complex separation dynamic mechanisms while the unsteady flow analysis is implemented. Consequently, this method can simulate several multi-physic problems such as booster separation with higher accuracy than the conventional methods. The effectiveness of the proposed method is evaluated in modeling of real time joint separation in the presence of unsteady aerodynamics. In addition, the interface was validated by simulating a transonic store separation event compared with experimental data obtained by the authors [14].

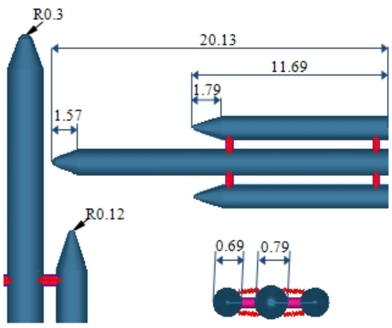

Figure 1. Launch vehicle configuration (meter)

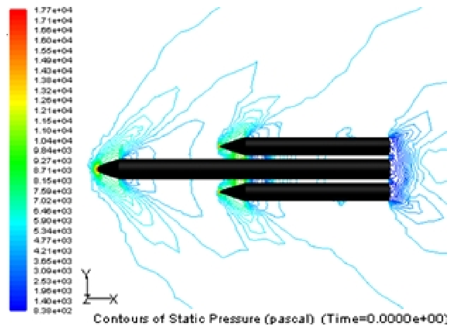

Figure 2. Pressure distribution around the launch vehicle before the separation

2. PROBLEM DESCRIPTION

The 6-DOF dynamic separation of the strap-on boosters from the fixed core using spring ejector mechanism and spherical joints is simulated. The external geometry of the launch vehicle with springs and joint positions are shown in Figure 1.

3. LAUNCH VEHICLE AERODYNAMIC WITH STRAP-ON BOSTERS

In order to calculate the aerodynamic forces and moments, a numerical solution of unsteady flow with an implicit up wind accurate 3D Euler solver is used. A dynamic unstructured tetrahedral mesh adoption approach using combination of spring-based smoothing [3] and local remeshing [4] is automatically employed with respect to bodies motion and determines the location of new nodes. In this analysis, the entire field is totally divided into about 900000 tetrahedral cells. Separation process is done at the altitude of 21 km with 4728.9 kPa gage pressure at Mach 1.6, and the air flow around the launch vehicle is assumed perfect gas. The pressure distribution in the flow field around the launch vehicle and strap-on boosters before the separation can be seen in Figure 2.

3. 1. Flow Solver Validation

As a validation of flow solver, wind tunnel data of the Titan-IV was used (Figures 3, 4). In this test, the free stream Mach number is 1.6, the angle of attack is zero and the separation height is 36000 meters. In Figure 3, the calculated pressure contour for Titan-IV cross section is shown. Good agreement between the numerical solution and the wind tunnel results can be observed in most regions. Slight differences of the connecting points of the core rocket and boosters are because of a connecting cable in the wind-tunnel test.

3. 2. Mesh Independence

Pressure changes in the longitudinal direction of the main body of the launch vehicle (before separation) were calculated for different mesh sizes. Three samples of these changes can be seen in Figure 5. The calculated pressures are roughly similar in both normal and fine cases, so the normal mesh size of about 900000 cells has been selected.

4. BOOSTERS SEPARATION DYNAMICS

The booster separation dynamics is derived using the constraint force equation (CFE) methodology. The CFE methodology provides a framework to compute the internal forces and moments acting on two bodies with specified degrees of freedom and apply them as external forces and moments to each body. Then, the motion of each body can be simulated independently like multiple free bodies. Thus, CFE methodology provides the missing link to model the stage separation [15, 16].

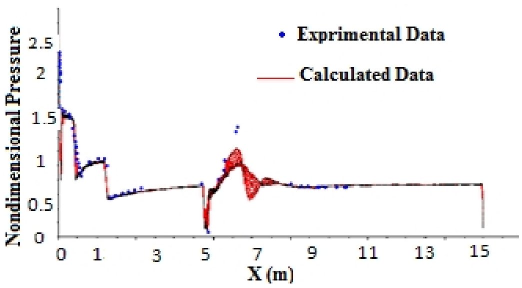

Figure 3. Comparison of computed surface pressure with wind-tunnel data along the centerline

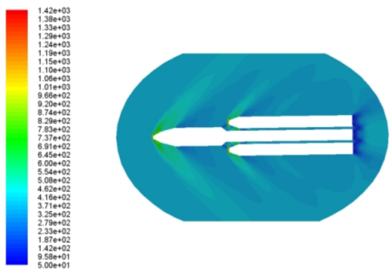

Figure 4. Pressure contour around the Titan-IV launch vehicle

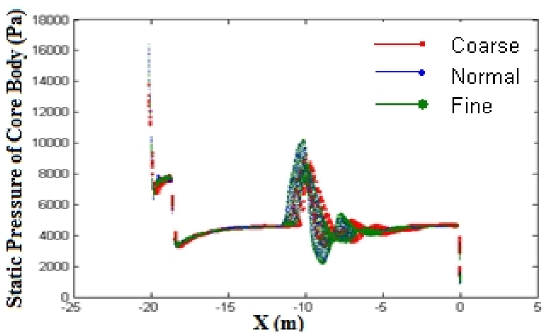

Figure 5. Computed surface pressure along the centerline for different grid sizes

4. 1. Separation Mechanisms Model

4. 1. 1. Separation Springs The equation used to calculate the spring force is:

$$Fs = -C\left(\frac{db}{dt}\right) - K(r\text{-}L_0) + F_{max} \quad (1)$$

in which

K= spring stiffness

C= viscous damping ratio

R= spring displacement

L_0 = spring initial length

F_{max} = spring initial length

The linear spring initial length is chosen as 0.9762 m, the initial force is 5000 N and the stiffness coefficient is 27000 N/m^2. When spring comes into force 450 N (spring stroke is 0.167 meters), separates from the launch vehicle and its force becomes zero.

4. 1. 2. Spherical Constraint Joints Modeling Spherical constraint joints were applied to connect the boosters on the launch vehicle. For any constraint, ball and socket attachments were allocated. One of these attachments was connected to the booster (ball) and the other one was connected to the body of vehicle. The applied constraints were spherical, so the translational motion of them was limited in three dimensions, wherein there was no interference with the rotational motion. If A is pointed to the joint on the vehicle and B is pointed to the same location on the booster, one can obtain:

$$\begin{Bmatrix} D_x(A,B)=0 \\ D_y(A,B)=0 \\ D_z(A,B)=0 \end{Bmatrix} * C_{sep} \quad (2)$$

in which the zero function (C_{sep}) is:

$$C_{sep} = \begin{cases} 1 & time \le 0.001 \ sec \\ 0 & time \ge 0.001 \ sec \end{cases}$$

Because of the above equation, joint$_1$ (refer to Figure 1, right booster, up) separates from launch vehicle after 0.001 sec. The angle condition was used to disconnect the two afterward attachments. When the relative angle between booster and vehicle body reaches to one deg, the joint is disconnected.

$$C_{sep} = \begin{cases} 1 & (\psi_{booster} - \psi_{main}) \le 1 \ deg \\ 0 & (\psi_{booster} - \psi_{main}) \ge 1 \ deg \end{cases}$$

It is noticeable that in the present plan, all of the constraints and springs have the same cross sectional areas, so the corresponding spring of any constraints are not contributed to the solution, until the separation of the constraint occurs. This fact results that, the operation of springs at the lower section, begins at t=0.09 sec. The block diagram of this solution can briefly be seen in the following graph. According to this algorithm, the code calculating the dynamic of the motion reports the position of vehicle to the flow solver, so the solver could derive the aerodynamic forces and moments in each time step. Using the results of forces and moments, this code calculates the linear and angular velocities of the vehicle. Consequently, the mesh is corrected in the next step. In this algorithm, both dynamic and aerodynamic solvers are connected to the main interface as two independent external functions.

TABLE 6. Mass properties

Launch vehicle	Strap-on booster
M : 22800.0 kg	M : 2000.0 kg
IXX : 7000.0 kg-m^2	IXX : 477.0 kg-m^2
IYY : 700000.0 kg-m^2	IYY : 19077.0 kg-m^2
IZZ : 700000.0 kg-m^2	IZZ : 19077.0 kg-m^2
IXY : 0.0 kg-m^2	IXY : 0.0 kg-m^2
IZX : 0.0 kg-m^2	IZX : 0.0 kg-m^2
IYZ : 0.0 kg-m^2	IYZ : 0.0 kg-m
Without initial speed	Without initial speed

TABLE 7. Characteristics of spring separation mechanism (springs 1, 2, 5 and 6 in forward section and springs 3, 4, 7 and 8 in aft section)

Spring ejectors	Number: 1, 2, 5 and 6 (forward)	Number:7, 4, 3 and 8 (aft)
Type	Translational	Translational
Damping coef	0.0 N-S/m	0.0 N-S/m
Stiffness	27000.0 N /m	27000.0 N /m
Initial force	5000.0 N	1800.0 N
Initial distance	0.9762 m	0.9762 m

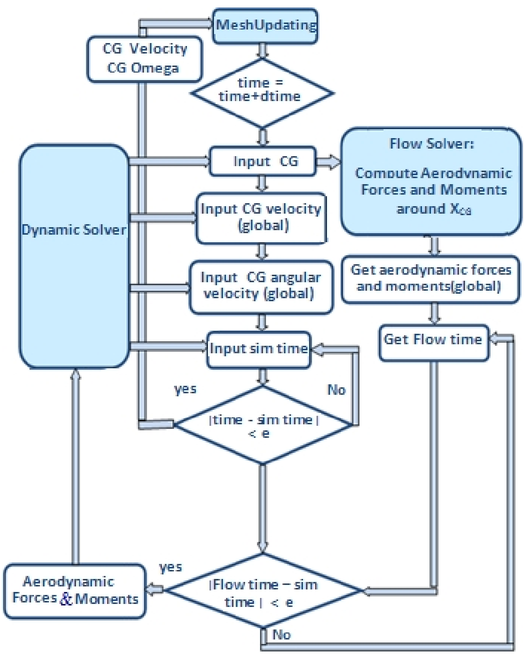

Figure 6. The block diagram of dynamic and aerodynamic coupling

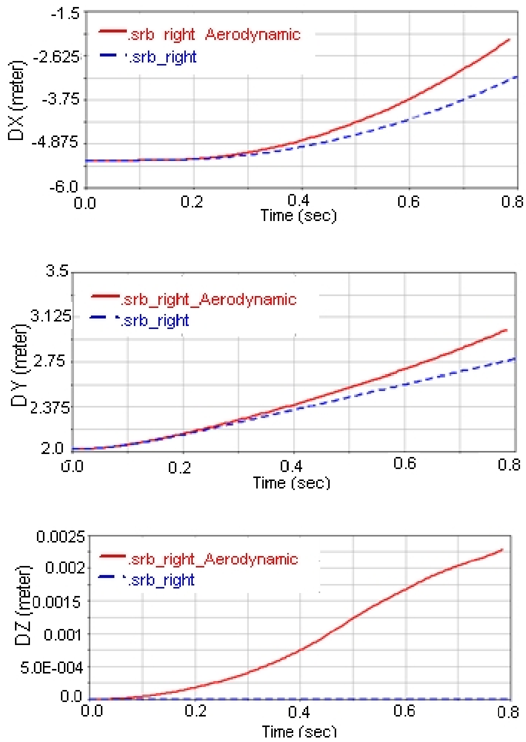

Figure 7. Variation of the right booster relative distances, ΔX, ΔY and ΔZ (relative to the core CM) with time during separation, in the presence of aerodynamic effects and without them

5. RESULTS

The results are given for the first 0.8 seconds of the motion, with aerodynamic effects and without them. All graphs are plotted for the left booster and the right booster, while the core rocket is fixed. In Figures 7 and 8, the relative distance between booster's center of mass and core rocket are observed (ΔX and ΔY and ΔZ) with aerodynamic effects and without them. Without aerodynamic effects, there is no displacement in the z direction and the motion is in XY plane. Figure 9 shows the relative speeds of left and right booster center of mass, (ΔX, ΔY and ΔZ), with aerodynamic effects and without them. According to this figure, the aerodynamic effect on the separation rate clearly and the velocity along the X and Y directions, respectively increases about 30 and 50 percent. Considering that joints are active for approximately 0.15 seconds and spring ejectors for 0.3 seconds, therefore, without considering the aerodynamic effects, velocity in separation direction (Y) remains constant after 0.3 seconds. It can be seen by translational acceleration in Figure 10. In Figure 11, angular velocities, p, q and r, for the left and right boosters are presented with and without the aerodynamic effects. The angular rate (r) increases from about 0.15 seconds but because of the joints disconnection and (aft) spring ejectors action, this rate decreases. Finally, after 0.3 seconds, spring ejectors are separated and only aerodynamic effects cause rotation. So without aerodynamic effects consideration, angular velocity remains constant. The aerodynamic forces and moments variation with time can be seen in Figures 12 and 13 for the left and the right boosters, respectively. In Figure14, the pressure couture variation during booster separations and the moments of separation process are presented. The Bow shocks effect created in the top and the bottom of boosters as ejector forces can be seen in this figure. In this case, the spherical joints in the forward section cut off at 0.001 seconds after separation start. Therefore, the boosters begin to rotate about (aft) joints until the boosters reach to the angle of 1 degree (about z-axis) and then aft joints separate from the core rocket.

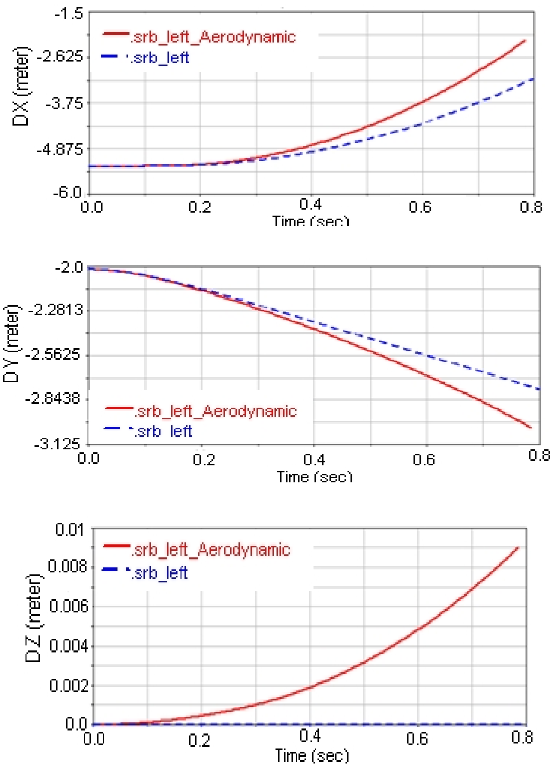

Figure 8. Variation of the left booster relative distances , ΔX, ΔY and ΔZ (relative to the core CM) with time during separation, in the presence of aerodynamic effects and without them

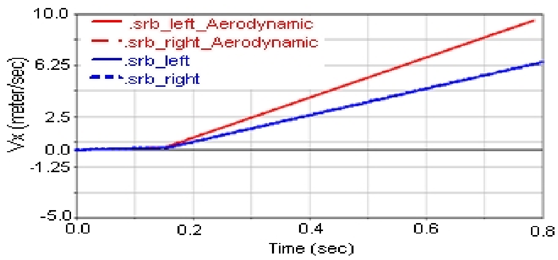

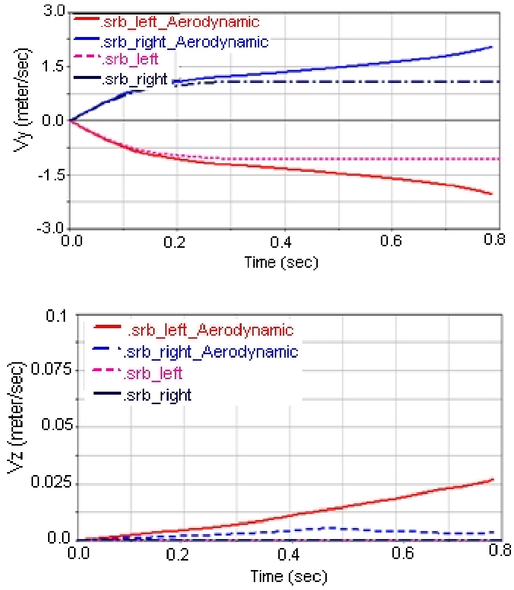

Figure 9. Variation of the left and right boosters relative velocities, ΔVx, ΔVy and ΔVz (relative to the core CM) with time during separation, in the presence of aerodynamic effects and without them

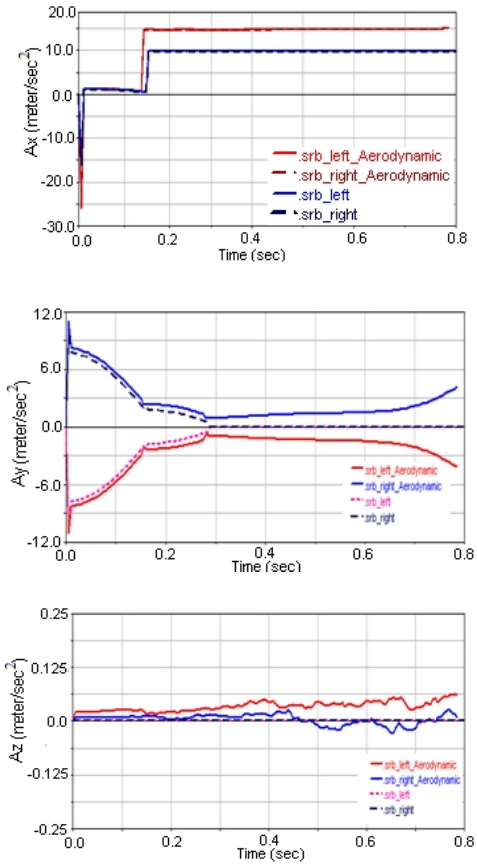

Figure 10. Variation of the left and right boosters relative translational accelerations, Ax, Ay and Az (relative to the core CM) with time during separation, in the presence of aerodynamic effects and without them

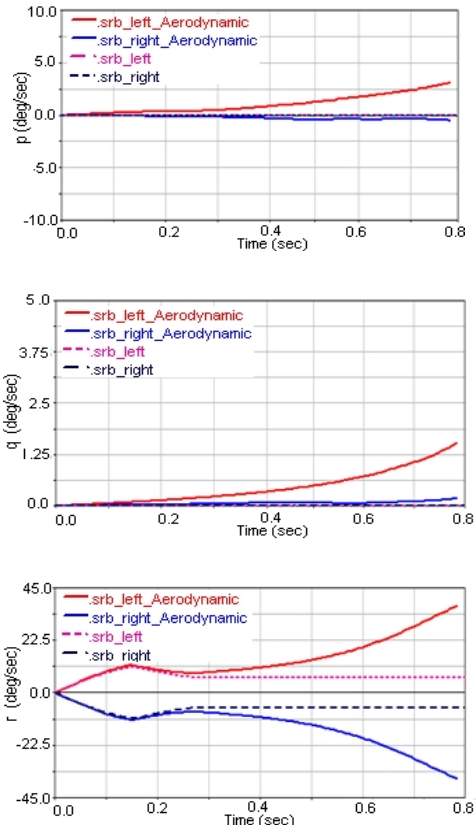

Figure 11. Variation of the left and right boosters angular velocities, p, q and r with time during separation, in the presence of aerodynamic effects and without them

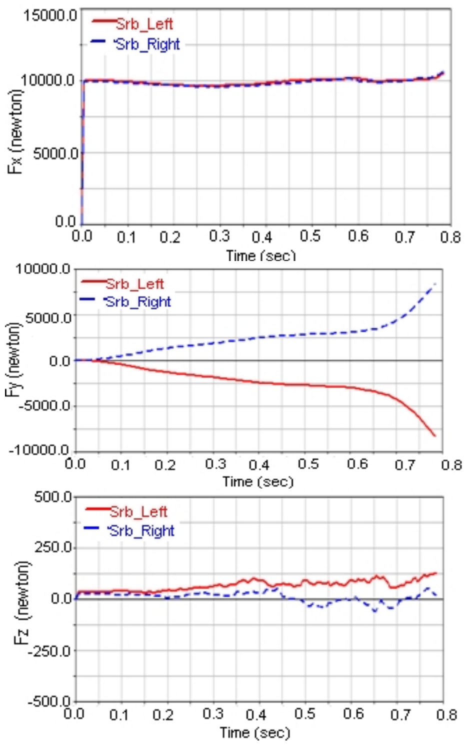

Figure 12. Variation of aerodynamic forces with time on left and right boosters

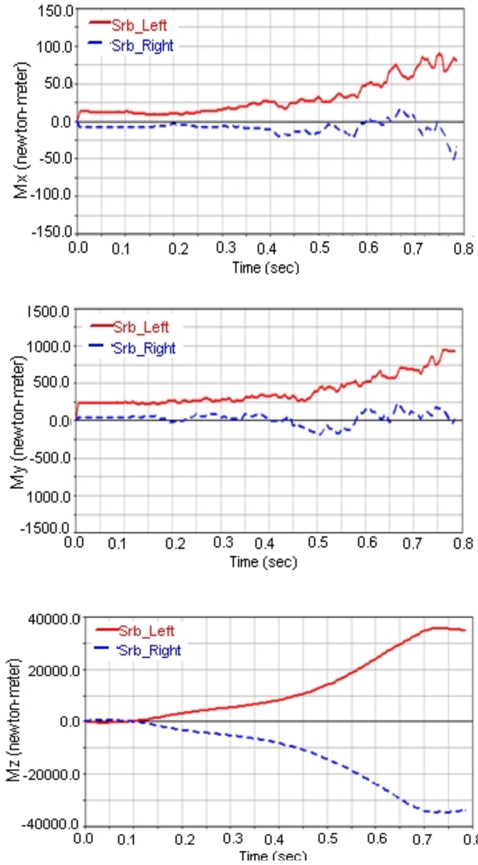

Figure 13. Variation of aerodynamic moments with time on left and right boosters

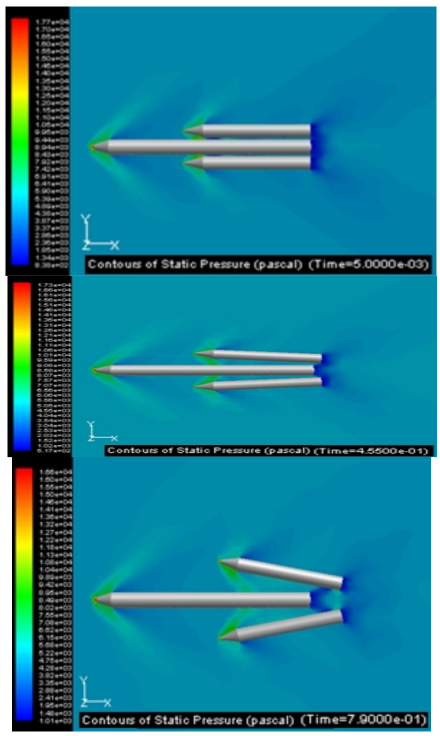

Figure 14. Pressure contour variation around the launch vehicle during strap-on boosters separation

6. CUNCLUSION

In this study, 6-DOF strap-on boosters separation from the launch vehicle was presented. In addition to spring ejector mechanisms and constraint joints, aerodynamic forces and moments were considered using coupled constraint dynamics and numerical aerodynamics. As mentioned, the strap-on boosters separation from launch vehicle has already been studied in the literature, but to the best of author's knowledge, in the entire previous works just one of the dynamic motions or flow aerodynamics was simulated precisely and the others were modeled simply or as prescribed.

In this paper, the first version of the software code, named IRASEP, was presented for real-time simulation of coupled dynamics and aerodynamics of constrained strap-on boosters from launch vehicle. The ability of this interface software in connection of multi-body dynamics solver and the numerical aerodynamic solver has provided a high potential in separation simulation in the dense atmosphere.

In this simulation, two time-dependent solvers of unsteady dynamics and aerodynamics are completely independent of each other and just exchange the information through an interface software. Thus, more accurate modeling of dynamic mechanisms in the presence of unsteady aerodynamics is possible compared to conventional methods. The proposed method is proved by real-time simulation of joints in separation in the presence of unsteady aerodynamics as an example that none of the references has provided it so far. Considering diagrams and separation animations, the importance of aerodynamic effects in strap-on booster separation simulation is quite evident.

7. REFERENCES

1. Meakin, R.L. and Suhs, N.E., "Unsteady aerodynamic simulation of multiple bodies in relative motion", ***AIAA Paper***, Vol. 1996, (1989).
2. Lochan, R., Adimurthy, V. and Kumar, K., "Separation dynamics of strap-on boosters in the atmosphere", ***Journal of Guidance, Control, and Dynamics***, Vol. 20, No. 4, (1997), 633-639.
3. Lijewski, L.E. and Suhs, N.E., "Time-accurate computational fluid dynamics approach to transonic store separation trajectory prediction", ***Journal of Aircraft***, Vol. 31, No. 4, (1994), 886-891.
4. Taylor, S. and Wang, J.C., "Launch-vehicle simulations using a concurrent, implicit navier-stokes solver", ***Journal of Spacecraft and Rockets***, Vol. 33, No. 5, (1996), 601-606.
5. E Azevedo, J., Jr, P.M., Maliska, C., Marchi, C. and C. Silva, A., "Code validation for high-speed flow simulation over satellite launch vehicle", ***Journal of Spacecraft and Rockets***, Vol. 33, No. 1, (1996), 15-21.
6. Ko, S.-H. and Kim, C., "Separation motion of strap-on boosters with base flow and turbulence effects", ***Journal of Spacecraft and Rockets***, Vol. 45, No. 3, (2008), 485-494.
7. Snyder, D.O., Koutsavdis, E.K. and Anttonen, J.S., "Transonic store separation using unstructured cfd with dynamic meshing", ***AIAA paper***, Vol. 3919, (2003).
8. Murman, S.M., Aftosmis, M.J. and Berger, M.J., "Simulations of 6-dof motion with a cartesian method", ***AIAA Paper***, Vol. 1246, (2003).
9. Pamadi, B. N., Hotchko, N. J., Samareh, J., Covell, P. F. and Tartabini, P. V., "Simulation and analyses of multi-body separation in launch vehicle staging environment", 14th AIAA/AHI Space Planes and Hypersonic Systems and Technologies Conference AIAA, Vol. 803, (2006).
10. Murphy, K.J., Buning, P.G., Pamadi, B.N., Scallion, W.I. and Jones, K.M., "Overview of transonic to hypersonic stage separation tool development for multi-stage-to-orbit concepts", ***AIAA paper***, Vol. 2595, (2004).
11. Pamadi, B.N., Neirynck, T.A., Covell, P.F., Hotchko, N. and Bose, D., "Simulation and analyses of staging maneuvers of next generation reusable launch vehicles", ***AIAA Paper***, Vol. 5185, (2004).
12. Pamadi, B.N., Neirynck, T.A., Hotcko, N.J., Scallion, W.I., Murphy, K.J. and Covell, P.F., "Simulation and analyses of stage separation of two-stage reusable launch vehicles", ***Journal of Spacecraft and Rockets***, Vol. 44, No. 1, (2007), 66-80.
13. Pamadi, B. N., Tartabini, P. V., Toniolo, M. D., Roithmayr, C. M., Karlgaard, C., and Samareh, J "Application of CFE/POST2 for simulation of launch vehicle stage separation", ", NASA Langley Research Center, Hampton VA 23681.
14. Jafari, M., Toloei, A., Ghasemlu, S. and Parhizkar, H., "Simulation of store separation using low-cost cfd with dynamic meshing", ***International Journal of Engineering-Transactions B: Applications***, Vol. 27, No. 5, (2013), 775-784.
15. Toniolo, M.D., Tartabini, P.V., Pamadi, B.N. and Hotchko, N., "Constraint force equation methodology for modeling multi-body stage separation dynamics", ***AIAA Paper***, Vol. 219, (2008).
16. Tartabini, P.V., Roithmayr, C., Toniolo, M.D., Karlgaard, C. and Pamadi, B.N., "Verification of the constraint force equation methodology for modeling multibody stage separation", ***AIAA Paper***, Vol. 7039, (2008).

Simulation of Strap-on Boosters Separation in the Atmosphere

M. Jafari[a], A. Toloei[a], S. Ghasemlu[b], H. Parhizkar[b]

[a]*Department of New Technologies Engineering, ShahidBeheshti University, Tehran, Iran*
[b]*Space Research Institute, Tehran, Iran*

P A P E R I N F O

Paper history:
Received 04 July 2014
Received in revised form 07 October 2014
Accepted 13 November 2014

Keywords:
Strap-on Boosters Separation
Numerical Dynamic-aerodynamic Interface
Constraint Force Equation Methodology

چکیده

در مقاله حاضر یک کد نرم افزاری واسط برای شبیه سازی همزمان دینامیک و آیرودینامیک بوسترهای جانبی مقید، از ماهواره‌بر در جو غلیظ ارائه گردیده است. به این منظور، یک حل‌گر شش درجه آزادی دینامیک چند جسمی، با استفاده از متد معادله نیروی قید، به یک حلگر عددی وابسته به زمان جریان اویلر کوپل شده است. در این شبیه سازی، از یک روش به روز رسانی شبکه متحرک به کمک روش هموارسازی فنری و تجدید شبکه موضعی، برای تطبیق حرکت جسم در میدان محاسباتی گسسته، به صورت خودکار استفاده شده است. کد واسط ارائه شده در این مقاله، قادر به شبیه سازی جدایش چند جسم با مدل سازی کامل مکانیزم های جدایش مانند فنرهای جدایش، تراسترها، مفاصل و غیره در حضور اثرات آیرودینامیک جریان می‌باشد. حل‌گر جریان با کمک نتایج تست تونل باد بر روی ماهواره‌بر تیتان٤ صحت سنجی شده و بیانگر دقت مناسب آن می‌باشد. در پایان، شبیه سازی جدایش برای یک ماهواره‌بر نمونه با دو بوستر جانبی و با بکارگیری سیستم جدایش فنری و اتصالات مفصلی در اتمسفر غلیظ ارائه شده است. بنابراین، ویژگی کد واسط ارائه شده در این تحقیق را می‌توان امکان شبیه‌سازی همزمان مکانیزم‌های پیچیده دینامیک جدایش در حضور آیرودینامیک عددی ناپایا، دانست.

***doi**: 10.5829/idosi.ije.2015.28.02b.01*